Synchrotron x-ray photoelectron spectroscopy study of hydrogen-terminated 6*H*-SiC{0001} surfaces

N. Sieber, Th. Seyller,* and L. Ley
Institut für Technische Physik, Lehrstuhl für Experimentalphysik, Universität Erlangen-Nürnberg, Erwin-Rommel-Strasse 1, 91058 Erlangen, Germany

D. James, J. D. Riley, and R. C. G. Leckey
Department of Physics, La Trobe University, Bundoora, Victoria 3083, Australia

M. Polcik
Fritz-Haber-Institut, Faradayweg 4-6, 14195 Berlin, Germany
(Received 31 October 2002; revised manuscript received 28 February 2003; published 6 May 2003)

We report on highly resolved core-level and valence-band photoemission spectroscopies of hydrogenated, unreconstructed 6*H*-SiC(0001) and $(000\bar{1})$ using synchrotron radiation. In the C 1*s* core level spectra of 6*H*-SiC$(000\bar{1})$ a chemically shifted surface component due to C-H bonds is observed at a binding energy (0.47 ± 0.02) eV higher than that of the bulk line. The Si 2*p* core-level spectra of SiC(0001) suggest the presence of a surface component as well but a clear identification is hindered by a large Gaussian width, which is present in all spectra and which is consistent with values found in the literature. The effect of thermal hydrogen desorption was studied. On 6*H*-SiC(0001) the desorption of hydrogen at 700–750 °C is accompanied by a simultaneous transformation to the Si-rich $(\sqrt{3}\times\sqrt{3})R30°$ reconstruction. On 6*H*-SiC$(000\bar{1})$ first signs of hydrogen desorption, i.e., the formation of a dangling bond state in the fundamental band gap of SiC, are seen at temperatures around 670 °C while the (1×1) periodicity is conserved. At 950 °C a (3×3) reconstruction is formed. The formation of these reconstructions on thermally hydrogenated 6*H*-SiC(0001) and $(000\bar{1})$ is discussed in the light of earlier studies of 6*H*-SiC{0001} surfaces. It will be shown that by using the hydrogenated surfaces as a starting point it is possible to gain insight into how the $(\sqrt{3}\times\sqrt{3})R30°$ and (3×3) reconstructions are formed on 6*H*-SiC(0001) and 6*H*-SiC$(000\bar{1})$, respectively. This is due to the fact that only hydrogen-terminated 6*H*-SiC{0001} surfaces possess a surface carbon to silicon ratio of 1:1.

DOI: 10.1103/PhysRevB.67.205304 PACS number(s): 68.35.Bs, 68.43.Fg, 68.43.Jk

I. INTRODUCTION

In the past years a number of investigations on the properties of hexagonal {0001} surfaces of 6*H*- and 4*H*-SiC have been reported. A majority of these studies dealt with the Si-rich[1–10] (3×3) and $(\sqrt{3}\times\sqrt{3})$R30° (Refs. 6–24) reconstructions on 4*H*- and 6*H*-SiC(0001), the (3×3) reconstruction[5,25] on 6*H*-SiC$(000\bar{1})$, and the oxygen induced silicate adlayer reconstructions on 4*H*- and 6*H*-SiC{0001} surfaces.[7,9,10,26–32] These surface reconstructions have in common that their surface energy is minimized via a reduction of the total number of dangling bonds at the surface. This is achieved by an ordered accumulation of surplus oxygen and/or silicon atoms at the surface, which consequently results in a deviation of the surface composition from the bulk stoichiometry. Nevertheless, many of these surfaces still possess dangling bonds that make them extremely susceptible to oxidation. In contrast, silicate adlayer reconstructed surfaces show an extraordinary stability in air. However, the silicate adlayer is also thermally stable up to temperatures of about 1000 °C, which makes this termination problematic for applications where an oxide interface layer is not desired. As a consequence, the above-mentioned surface reconstructions seem not to be adequately suited as basis for the development of SiC semiconductor devices.

A convenient way to prepare clean and unreconstructed SiC surfaces would be a wet-chemical treatment such as that used in Si technology, where the so-called RCA (Radio Corporation of America)[60] clean followed by a dip in buffered HF is a commonly employed technique. The procedure yields extremely flat Si surfaces which are unreconstructed and terminated by hydrogen. The strong Si-H bonds remove surface states from the gap leading to extremely low densities of charged surface defects. Yablonovitch *et al.*[33] reported a record low of 2.5×10^7 charged surface states per cm^2 for hydrogenated Si(111). In addition, the hydrogen-terminated Si surfaces are relatively well protected against oxidation in air.[33,34] Although the (0001) surface of the hexagonal polytypes 6*H*-SiC and 4*H*-SiC is crystallographically equivalent to Si(111), the surface chemistry is different on account of the additional carbon atoms. Dipping these surfaces in HF leaves them covered with hydroxyl groups,[32,35,36] and annealing to temperatures above 950 °C is necessary to remove the oxygen from the wet-chemically prepared surface.[13] In addition, they are usually contaminated with hydrocarbons as well, which may decompose partially at elevated temperatures. The wet-chemical procedure also fails for the $(000\bar{1})$ surfaces for similar reasons.[32,37]

The only method to yield SiC{0001} surfaces saturated with a monolayer of hydrogen was first suggested by Tsuchida *et al.*,[38–41] who have annealed their samples in an atmosphere of ultraclean hydrogen at temperatures of

 ©2003 The American Physical Society

1000 °C and higher. This procedure is similar to the hydrogen etching which is widely used to reduce surface roughness and polishing damage of SiC substrate surfaces prior to homoepitaxial growth by chemical vapor deposition (CVD).[42,43] In previous studies[44–48] we have investigated the chemical, electronic, and structural properties of 6*H*-SiC{0001} surfaces that were hydrogenated by the method of Tsuchida *et al.* The hydrogenated surfaces with (1×1) periodicity were observed to be free of unwanted contaminations such as oxygen and hydrocarbons.[44] We were also able to show that the density of charged defects on SiC(0001) can be pushed down to values of 7×10^{10} cm^{-2} and below and that the surfaces are stable against oxidation in air.[44] These observations suggest that hydrogenation of SiC{0001} surfaces by high-temperature hydrogen annealing is an adequate method for surface preparation especially because it can be carried out in a CVD reactor directly after homoepitaxial growth, which is usually performed for many device applications.

Another interesting aspect of the hydrogen passivated SiC{0001} surfaces is that they are the only known terminations of SiC where the Si to C ratio is equal to the bulk ratio 1:1. Therefore it seemed worthwhile to study the hydrogenated SiC{0001} surfaces in more detail. We have employed highly resolved photoelectron spectroscopy using synchrotron radiation in order to study the core-level and valence-band spectra of both 6*H*-SiC(0001) and $(000\bar{1})$ in the as-prepared state as well as after annealing in UHV, which induces a change in surface periodicity from (1×1) to $(\sqrt{3}\times\sqrt{3})R30°$ or (3×3), respectively. As we will show in the following sections, the fact that the initial stoichiometry of the hydrogenated surfaces is equal to the bulk stoichiometry provides important insights into how these recostructions are formed and into the origin of the surface components observed in the Si $2p$ and C $1s$ core level spectra of these reconstructions.[13,23,25]

The present paper is organized in the following way. After a brief description of our experimental procedures in Sec. II we will discuss our results in Sec. III. Thereby a short structural characterization using low-energy electron diffraction (LEED) and Fourier-transform infrared-absorption spectroscopy in attenuated total reflection mode (FTIR-ATR) will be presented in Sec. III A. Sections III B and III C contain a detailed analysis of highly resolved synchrotron x-ray photoelectron spectroscopy measurements on the hydrogenated 6*H*-SiC{0001} surfaces. This is followed by a discussion of the inelastic mean free paths determined from our experiments (Sec. III D). Thermally induced hydrogen desorption and subsequent formation of $(\sqrt{3}\times\sqrt{3})R30°$ and (3×3) on 6*H*-SiC(0001) and $(000\bar{1})$, respectively, will be the topic of Secs. III E and III F. Finally, our conclusions are presented in Sec. IV.

II. EXPERIMENTAL

The investigations were focused on the basal planes of 6*H*-SiC. These are the Si-terminated SiC(0001) surfaces, which are also called silicon faces, and the C-terminated SiC$(000\bar{1})$ surfaces (carbon faces). The Si-terminated samples from CREE Research, Inc. were either 3.5° off-axis oriented, polished substrates, or homoepitaxial epilayers, with a doping of 1.4×10^{18} cm^{-3} (n type) and 1×10^{16} cm^{-3} (p type), respectively. The C-terminated crystals from SiCrystal were n type (5×10^{18} cm^{-3}) and polished on-axis.

Before hydrogenation the samples were subjected to a four-step wet-chemical cleaning procedure using hydrofluoric acid and mixtures of sulphuric acid, hydrogen peroxide, and hydrochloric acid as described elsewhere.[32,35] Hydrogen termination was achieved by annealing the samples in ultrapure hydrogen (8.0) at temperatures around 1000 °C and a pressure of 1×10^{5} Pa using a contactless infrared heating system. The base pressure of the UHV preparation chamber was below 5×10^{-7} Pa. A transportable vacuum storage chamber equipped with a mobile ion pump (base pressure below 1×10^{-6} Pa) allowed to transfer up to six hydrogenated samples to the measuring chambers in our home laboratories for investigations with LEED and x-ray induced photoelectron spectroscopy (XPS). In addition, the samples were also investigated with FTIR-ATR. These measurements were carried out *ex situ* using a Ge prism as multiple internal reflection element.

Using the aforementioned vacuum transport system, the samples could be transferred to the synchrotron radiation source BESSY II and load locked to the UHV system without breaking the vacuum. Highly resolved photoelectron spectroscopy was carried out at the undulator beam line UE56/2-PGM 2. The end station with a base pressure below 1×10^{-8} Pa was equipped with a hemispherical analyzer and a LEED optics. In order to achieve a contrast in surface sensitivity, photon energies of 170 eV and 350 eV were applied to investigate the Si $2p$ core levels and 350 and 510 eV to investigate the C $1s$ core levels. A photon energy of 74 eV

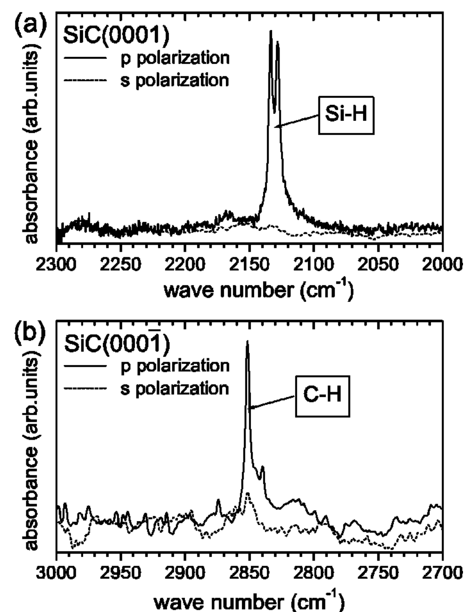

FIG. 1. *Ex situ* FTIR-ATR spectra of hydrogen terminated 6*H*-SiC(0001) (a) and 6*H*-SiC$(000\bar{1})$ (b).

was used for the valence-band measurements. A polar angle (electron escape angle) of $\theta = 20°$ was used to measure the core-level spectra and of $\theta = 0°$ for the valence-band spectra. The experimental resolution was better than 100 meV, 150 meV, 240 meV, and 300 meV for photon energies of 74 eV, 170 eV, 350 eV, and 510 eV, respectively, as derived from gold Fermi edges.

Thermally induced hydrogen desorption and subsequent surface reactions were studied by annealing the surfaces in UHV to temperatures up to 950 °C. Heating of the samples was accomplished by electron bombardment of the backside of the sample holder. The annealing temperature was monitored by means of a pyrometer with the emissivity adjusted to that of the sample holder made of molybdenum ($\epsilon = 0.25$). Standard annealing time was 2 min. Calibration measurements using a Ni/Cr-Ni thermocouple have shown that the temperature accuracy is about 30 °C. The effect of annealing in UHV was studied by photoelectron spectroscopy and Fourier-transform infrared-absorption spectroscopy.

III. RESULTS AND DISCUSSION

A. Structural characterization of the *H*-terminated 6*H*-SiC{0001} surfaces

Using photoelectron spectroscopy it is not possible to detect the hydrogen on the as-prepared 6*H*-SiC{0001} surfaces. Therefore hydrogenated samples were studied using Fourier-transform infrared-absorption spectroscopy in the attenuated total reflection mode. Figure 1 displays spectra of the Si-H and the C-H stretch modes measured on 6*H*-SiC(0001) and 6*H*-SiC(000$\bar{1}$), respectively. The C-H stretch mode on SiC(000$\bar{1}$) is located at (2851.5 ± 0.2) cm^{-1}, in good agreement with Tsuchida *et al.*[38–41] On SiC(0001), two Si-H stretch modes are observed at (2128.0 ± 0.6) cm^{-1} and (2133.5 ± 0.6) cm^{-1}, respectively. The splitting of the Si-H stretch mode, which has also been reported by Tsuchida *et al.*,[38–41] has been a subject of a detailed study[45] and was shown to be due to a small difference in the third-neighbor interactions of the Si-H dipole with the underlying lattice, which are different for Si-H units on cubic and hexagonally terminated terraces. The fact that C-H and Si-H stretch modes can only be observed in *p* polarization and not in *s* polarization (see Fig. 1) indicates that the Si-H and C-H bonds are perpendicular to the surface. Note also that only the monohydride configuration is clearly observable. Dihydrides or trihydrides are below the detection limit. In addition, no Si-H stretch mode signals were observed on SiC(000$\bar{1}$) and vice versa. The full width at half maximum values of the observed C-H and Si-H stretch mode signals are typically below 3.0 cm^{-1}, which points towards a high degree of order on the surfaces.

The high degree of surface order indicated by the small width of the Si-H and C-H stretch mode signals in Fig. 1 is corroborated by the corresponding LEED patterns of hydrogen covered 6*H*-SiC(0001) and 6*H*-SiC(000$\bar{1}$), which are displayed in Fig. 2. The surfaces exhibit a (1×1) periodicity with sharp diffraction spots. In addition, the LEED patterns show a remarkably low diffuse-elastic background which indicates well ordered surfaces. The results presented in this section will be helpful for the interpretation of the core-level spectra discussed below.

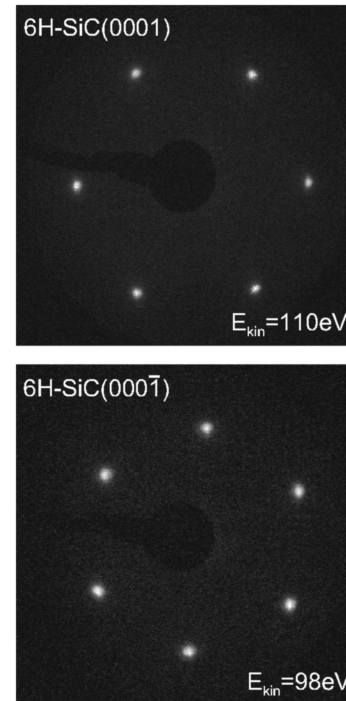

FIG. 2. (1×1) LEED images of hydrogen-terminated 6*H*-SiC(0001) (top) and 6*H*-SiC(000$\bar{1}$) (bottom). The azimuthal orientation was different for the two samples, as can be seen from the diffraction images.

B. Core-level spectra of hydrogenated 6*H*-SiC(000$\bar{1}$)

Figure 3(a) shows Si 2*p* core-level spectra of hydrogen-terminated 6*H*-SiC(000$\bar{1}$) measured at photon energies of 170 eV and 350 eV. As will be discussed in Sec. III D, the corresponding effective sampling depths are 3.0 and 4.6 Å, respectively. The binding energy is given with respect to the Si $2p_{3/2}$ bulk component, which was obtained by a peak fit routine as described later in this section. Despite the different surface sensitivity of the two measurements no variation of the line shape with photon energy is observed. For 6*H*-SiC(000$\bar{1}$):H the carbon atoms of the topmost bilayer, which constitute the surface, are saturated by a monolayer of hydrogen. Consequently, all silicon atoms below including those which are located in the same bilayer are chemically equivalent. It is thus not surprising that no chemically shifted component is observable in the Si 2*p* core level.

For a more detailed study, the core-level spectra were subjected to a nonlinear least-squares fitting analysis using a convolution of the Gaussian and Lorentzian line shapes, i.e., Voigt lines. The Gaussian width (ω_G) reflects the experimental resolution, the samples' inhomogeneity, and phonon broadening. The Lorentzian width (ω_L) is associated with the lifetime of the core hole which is generated by the photoionization process. Prior to curve fitting, a Shirley

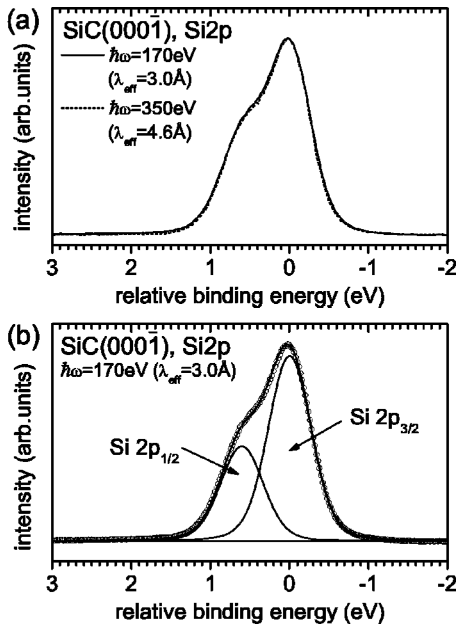

FIG. 3. Si $2p$ spectra of H-terminated $6H$-SiC$(000\bar{1})$. (a) Comparison of spectra taken at photon energies of 170 eV and 350 eV. (b) Deconvolution of the spectrum taken at a photon energy of 170 eV into one spin orbit split doublet.

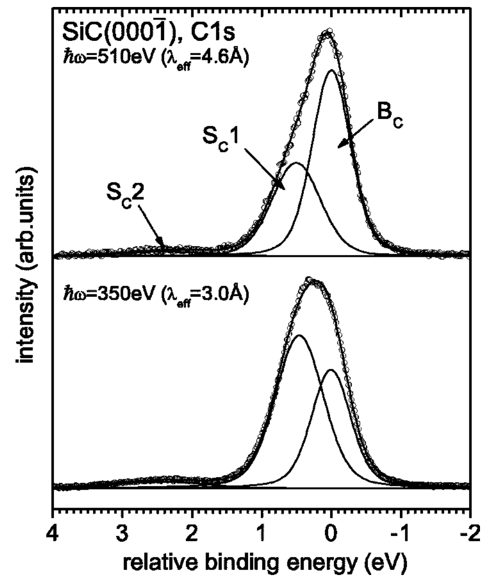

FIG. 4. C $1s$ spectra of hydrogen-terminated $6H$-SiC$(000\bar{1})$ taken at photon energies of 350 eV and 510 eV and their deconvolution.

background[49] was subtracted from the data. In all cases only marginal changes were noticeable when using a linear background instead of a Shirley background correction, implying that this has no effect on the results presented in this paper. The result of a peak fit applied to the Si $2p$ core-level spectrum of hydrogenated SiC$(000\bar{1})$ taken at 170 eV photon energy is displayed in Fig. 3(b). The spectrum can be fitted using a single spin-orbit split doublet. Table I summarizes the fit parameters for both, the 170-eV and the 350-eV spectrum. The only constraints used in the fit were that the Gaussian and Lorentzian widths of the Si $2p_{3/2}$ and Si $2p_{1/2}$ lines were forced to be equal, respectively. The spin-orbit splitting of the Si $2p_{3/2}$ and the Si $2p_{1/2}$ component was determined as (0.606 ± 0.003) eV and the branching ratio as 0.516 ± 0.004 within a data set of more than 15 Si $2p$ core levels, independent of surface sensitivity. The Lorentzian width was determined to be (0.128 ± 0.021) eV and the Gaussian width as (0.570 ± 0.030) eV, the latter value containing the largest experimental scatter since it depends on surface quality. The lowest Gaussian widths that were extracted from the fitting procedures were 0.53 eV, which is a reasonable value when compared with the lowest values given in the literature for SiC.[13,28]

TABLE I. Fit parameters obtained for the Si $2p$ core-level spectra of hydrogenated $6H$-SiC$(000\bar{1})$. SOS is the spin-orbit splitting and R$=I($Si $2p_{1/2}/I($Si $2p_{3/2})$ the branching ratio. ω_G and ω_L are the Gaussian and Lorentzian widths, respectively.

Si $2p$	$\hbar\omega=170$ eV $\lambda_{eff}=3.0$ Å	$\hbar\omega=350$ eV $\lambda_{eff}=4.6$ Å
SOS (eV)	0.606 ± 0.003	0.606 ± 0.003
R	0.514 ± 0.005	0.517 ± 0.002
ω_G (eV)	0.57 ± 0.02	0.56 ± 0.02
ω_L (eV)	0.14 ± 0.02	0.13 ± 0.01
Assigment	SiC bulk	SiC bulk

C $1s$ core-level spectra of the same hydrogenated $6H$-SiC$(000\bar{1})$ sample taken at photon energies of 350 eV and 510 eV are plotted in Fig. 4 together with their respective deconvolution. The sampling depths are identical to the ones used in the Si $2p$ core-level spectra shown in Fig. 3, i.e. 3.0 and 4.6 Å for photon energies of 350 and 510 eV, respectively. The shape of the main line varies clearly with photon energy, suggesting the presence of at least two components which is indeed expected on account of the terminating C-H bonds. The extremely weak intensity contribution at about 2.4 eV higher binding energy points to minute hydrocarbon contamination.

The C $1s$ core-level spectra of SiC$(000\bar{1})$:H could be fitted consistently using three Voigt lines, i.e., two lines ($B_{\rm C}$ and $S_{\rm C}1$) for the main contribution and one ($S_{\rm C}2$) for the weak contribution at about 2.4 eV higher binding energy, as shown in Fig. 4. The best-fit parameters are collected in Table II. The Gaussian widths were allowed to vary independently because of the different chemical origin of the lines. The Lorentzian widths were allowed to vary but set equal for all lines. Best fits were obtained for the Lorentzian widths of (0.19 ± 0.03) eV. This value is in good agreement with former reports on SiC and metal carbides.[50,51]

According to the way the relative intensities of the lines vary with changing surface sensitivity, the component at lowest binding energy (labeled $B_{\rm C}$ in Fig. 4) is ascribed to bulk SiC. The two other remaining components are due to emission from the surface. The component labeled $S_{\rm C}1$ in Fig. 4 with a chemical shift of (0.47 ± 0.02) eV towards

TABLE II. Fit parameters obtained for the C 1s core-level spectra shown of hydrogenated 6H-SiC(000$\bar{1}$). The binding energy is given with respect to the bulk component. $I(S_C1,2)/I(B_C)$ is the intensity ratio of the respective surface component (S_C1,2) to the bulk component (B_C).

C 1s	$\hbar\omega=350$ eV, $\lambda_{eff}=3.0$ Å			$\hbar\omega=510$ eV, $\lambda_{eff}=4.6$ Å		
Label in Fig. 4	B_C	S_C1	S_C2	B_C	S_C1	S_C2
E_b (eV)	0	0.46±0.02	2.44±0.10	0	0.48±0.02	2.41±0.11
$I(S_C1,2)/I(B_C)$		1.44±0.12	0.05±0.01		0.66±0.07	0.04±0.01
ω_G (eV)	0.58±0.03	0.71±0.03	1.48±0.12	0.55±0.03	0.72±0.02	1.47±0.11
ω_L (eV)	0.19±0.03	0.19±0.03	0.19±0.03	0.19±0.03	0.19±0.03	0.19±0.03
Assignment	SiC bulk	Si_3C-H	C_xH_y	SiC bulk	Si_3C-H	C_xH_y

higher binding energy is ascribed to the carbon atoms of the topmost bilayer, which form the surface C-H bonds seen in FTIR-ATR. Together with the Si atoms of the same bilayer their environment is Si_3C-H. The relative strength of this component was $I(S_C1)/I(B_C)=1.4(\pm 10\%)$ for surface sensitive and 0.7 ($\pm 10\%$) for less surface sensitive measurements on average. (An estimate whether these values are reasonable for a monolayer coverage of C-H bonds is given in Sec. III D). The bonding assignment is also qualitatively supported when the Pauling electronegativities of the three elements carbon, hydrogen, and silicon (2.6, 2.2, and 1.9, respectively) are considered. If one silicon atom is removed from a Si_4C tetrahedron (bulk SiC) and replaced by one hydrogen atom, the electronic configuration will change such that a smaller valence charge is transferred towards the carbon atom than before. This yields a higher binding energy of the carbon atom in a Si_3C-H environment. The Gaussian width of the bulk line (B_C) and the C-H component (S_C1) were determined as (0.57±0.03) eV and (0.71±0.03) eV, respectively. The former value compares well with that observed of the Si 2p core-level, which further supports our assignment. The Gaussian width of the C-H component (S_C1), however, is slightly larger, most probably on account of a different inhomogeneous broadening and/or phonon broadening.

The chemical shift of the small component S_C2 at higher binding energy in our C 1s core-level spectra (Fig. 4) was determined as (2.42±0.10) eV with respect to the bulk line and its Gaussian full width amounts to (1.48±0.13) eV. Based on its chemical shift of 2.4 eV, its surface sensitivity, and the large Gaussian width, this component is ascribed to weakly bound hydrocarbon contamination. Assuming that the density of adsorbed hydrocarbons is identical to that of liquid hydrocarbons (~0.75 kg/l), the average overlayer thickness can be estimated to be (0.1±0.05) Å when calculated with the effective sampling depths of $\lambda_{eff}=3.0$ and 4.6 Å for photon energies of 350 and 510 eV, respectively. This corresponds to ≈5% of a monolayer. The hydrocarbon contamination was observed to gradually increase with storage time of the samples in the vacuum transport system despite a pressure below 1×10^{-6} Pa. No contamination is usually detected directly after thermal hydrogen treatment by XPS in our home laboratory. There a similar surface sensitivity is achieved by a take-off angle of $\theta=75°$, which reduces the probe depth to about 4 Å. However, the beneficial effect of the vacuum transport system becomes evident when compared with *ex situ* measurements that exhibit at least ten times larger hydrocarbon contamination.[44]

C. Core-level spectra of hydrogenated 6H-SiC(0001)

Fig. 5(a) shows the surface sensitive ($\hbar\omega=170$ eV) and less surface sensitive ($\hbar\omega=350$ eV) Si 2p core-level spectrum of hydrogen saturated 6H-SiC(0001). For comparison the surface sensitive spectrum of the hydrogenated (000$\bar{1}$)

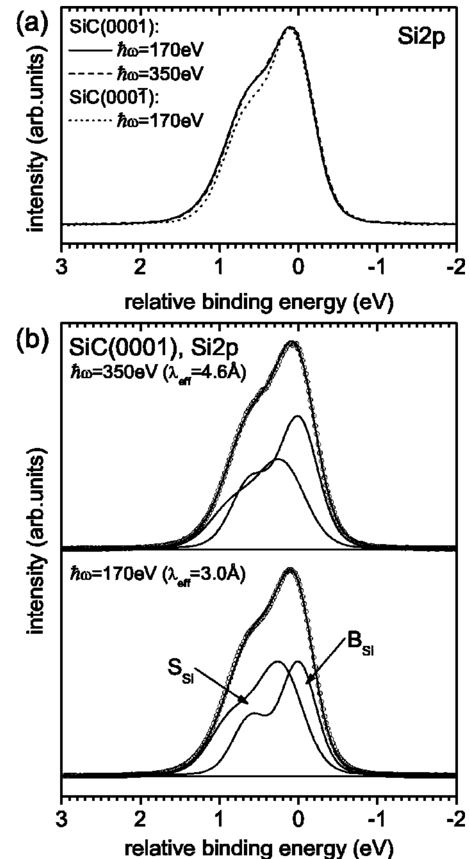

FIG. 5. (a) Si 2p spectra of hydrogenated 6H-SiC(0001) measured with high and low surface sensitivities in comparison with the surface sensitive spectrum of H-terminated 6H-SiC(000$\bar{1}$) from Fig. 3. (b) Deconvolution of the Si 2p spectra of hydrogenated 6H-SiC(0001) into two components.

TABLE III. Fit parameters obtained for the Si $2p$ core-level spectra of hydrogenated $6H$-SiC(0001). The binding energy is given with respect to the bulk component.

Si $2p$	$\hbar\omega = 350$ eV, $\lambda_{eff} = 3.0$ Å		$\hbar\omega = 510$ eV, $\lambda_{eff} = 4.6$ Å	
Label in Fig. 5	B_{Si}	S_{Si}	B_{Si}	S_{Si}
E_b (eV)	0	0.23 ± 0.02	0	0.21 ± 0.02
$I(S_{\mathrm{C}}1,2)/I(B_{\mathrm{C}})$		1.4		0.75
ω_G (eV)	0.48 ± 0.03	0.61 ± 0.03	0.51 ± 0.03	0.64 ± 0.03
ω_L (eV)	0.13 ± 0.02	0.13 ± 0.02	0.13 ± 0.02	0.13 ± 0.02
Assignment	SiC bulk	C_3Si-H	SiC bulk	C_3Si-H

surface from Fig. 3 is included in the plot. Although the presence of Si-H bonds on hydrogenated $6H$-SiC(0001) has been shown by FTIR-ATR (cf. Sec. III A), no chemically shifted component can be resolved in the Si $2p$ core-level spectra of $6H$-SiC(0001)-H. In addition, no variation of the line shape with sampling depths can be observed. On the other hand, the comparison of the Si $2p$ spectra of $6H$-SiC(0001):H with $6H$-SiC(000$\bar{1}$):H reveals two differences that were observed systematically within all experiments: first, the shoulder due to the spin-orbit splitting appears strongly enhanced and second, a slight asymmetry of the line shape towards the high binding-energy side becomes visible. As a consequence, the attempt to fit the Si $2p$ core-level spectra with only one spin-orbit split doublet, which led to good results on the carbon face, fails. It produces unreasonable values for the branching ratio and for the Lorentzian widths. The Si $2p$ line shape turned out to be independent of doping (p type or n type), surface quality (polished or epitaxial overgrown), and hydrogen coverage. These observations rule out differential charging or inhomogeneous surface band bending as well as surface defects as being responsible for the signal's odd shape. Phononic effects, which were suggested as an explanation for the asymmetric Si $2p$ core-levels of Si(111):H,[52] are also unlikely because we would expect their signature to be also visible in the spectra of the carbon face.

A possible explanation for the observed line shape would be to introduce a chemically shifted surface component due to Si atoms in a C_3Si-H environment. For a full monolayer coverage of Si-H bonds the intensity ratio of surface to bulk component should be similar to the one observed in the C $1s$ spectra of hydrogenated $6H$-SiC(000$\bar{1}$). Using this additional constraint the spectra can be fitted using two doublets as shown in Fig. 5(b). The corresponding fit parameters are compiled in Table III. With the constraints mentioned above, an energetic separation between the two components of (0.22 ± 0.02) eV is determined with the hydrogen induced surface component shifted to higher binding energy.

We note, however, that because of the identical line shape observed in the spectra taken with different photon energies, good quality fits can also be obtained by changing the assignment of the two components within the Si $2p$ line, i.e., inverting the intensity ratios. Considering the electronegativity of the elements Si, C, and H and assuming that initial-state effects are dominant, the hydrogen related component should be located at lower binding energy. However, we favor the opposite assignment where the component at higher binding energy corresponds to Si-H bonds for the following reasons. First, the Gaussian width of the component at higher binding-energy is larger than for the lower binding energy component. With SiC(000$\bar{1}$) the C-H component was also observed to be broader than the bulk line. Second, when considering the energetic separation between the bulk C $1s$ and Si $2p$ core-levels $[\Delta E = E(\mathrm{C}\ 1s) - E(\mathrm{Si}2p)]$, it is more likely that the assignment as shown in Fig. 5(b) is correct. In general we find values for $\Delta E = (182.17 \pm 0.05)$ eV for hydrogenated $6H$-SiC(000$\bar{1}$) independent of measuring device. For hydrogenated SiC(0001) surfaces we obtain values close to (182.19 ± 0.05) eV, when assigned as in Fig. 5(b). For the opposite assignment, the binding-energy difference is $\Delta E = (182.03 \pm 0.05)$ eV which appears somewhat too small. Nevertheless, we have to point out that our favored assignment cannot be confirmed with absolute confidence on the basis of our available dataset. In order to clarify this point measurements of better resolved core-level spectra are necessary, which could probably be achieved by cooling the sample to lower temperatures.

Corresponding C $1s$ core-level spectra of $6H$-SiC(0001) after hydrogenation are displayed in Fig. 6. Deconvolution of the spectra using only two components yields dissatisfactory results, hence we included a third component. The fit parameters are collected in Table IV. The strongest component (B_{C}) is due to emission from the bulk. A surface component labeled $S_{\mathrm{C}}2$ in Fig. 6 is located at about (2.2 ± 0.1) eV with respect to the bulk line. This component is attributed to weakly bound hydrocarbons. The component labeled $S_{\mathrm{C}}1$, which has to be included in order to fit the spectra properly, shows a chemical shift of (0.47 ± 0.03) eV in good agreement with the hydrogen induced surface component on SiC(000$\bar{1}$). Therefore, we propose that this component is due to carbon atoms at steps. Any SiC surface, independent of surface type (substrate, polished on- or off-axis or epitaxially overgrown), contains steps where necessarily surface carbon atoms are located. Additionally, any other surface imperfection contributes to the total number of surface carbon atoms. For our p-type epilayer, for example, we derive from atomic force microscopy (AFM) measurements a relative surface area of about 5% covered by steps. Of course, the question is why such a component was not observed in the Si $2p$ spectra of the carbon face, but in view of the small hy-

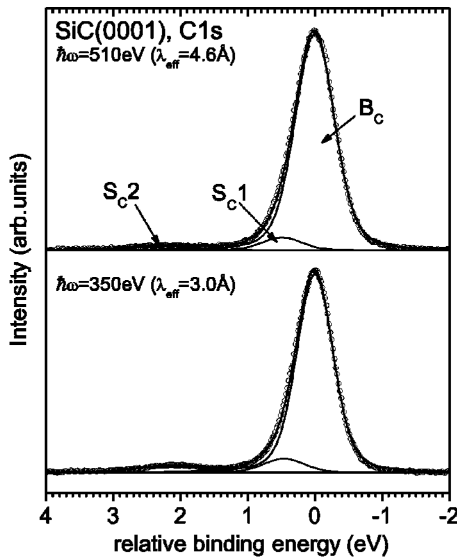

FIG. 6. C 1*s* spectra of hydrogen-terminated 6*H*-SiC(0001) taken at photon energies of 350 eV and 510 eV and their deconvolution.

drogen induced chemical shift of the Si 2*p* core-level it is reasonable that such a small component remains undetected.

D. Calculation of electron inelastic mean free path

As we have seen in Sec. III B the intensity ratio of surface C-H to bulk contribution in the C 1*s* core-level was determined as $I(\mathrm{Si_3C\text{-}H})/I(\mathrm{SiC}) = 1.4$ ($\pm 10\%$) for surface sensitive and 0.7 ($\pm 10\%$) for less surface sensitive measurements on the basis of the applied curve-fitting procedure. When a simple layer attenuation model is applied using the characteristic lengths of Si-C and C-H bonds we obtain the required ratios of 1.4 ($\hbar\omega = 350$ eV) and 0.7 $\hbar\omega = 510$ eV) for effective sampling depths of $\lambda_{eff} = 3.0$ and 4.6 Å, respectively. With an electron escape angle of $\theta = 20°$ this gives inelastic mean-free-path values of $\lambda = 3.2$ and 4.9 Å at kinetic energies of 60 and 220 eV, respectively. These numbers appear reasonable when compared with literature values of silicon, diamond, and silicon carbide (see Fig. 7). For silicon, minimum escape depths between 3.0 and 4.0 Å are reported for kinetic energies between 30 and 50 eV.[53,54] For diamond, somewhat lower escape depths are reported: 2.0–2.5 Å for (111) surfaces and 3.5 Å for (100) surfaces for electron kinetic energies between 35 and 40 eV.[55–57] For silicon carbide most publications refer to escape depths as they were obtained from quantitative calculations of silicon, and to our knowledge only Johansson *et al.*[13] estimated electron mean-free-path values for silicon carbide, albeit for higher kinetic energies. There values of 5.1 and 9.0 Å are obtained for kinetic energies of 450 and 650 eV, respectively. The listed literature values as well as our own results of further measurements in an extended photon energy range (not shown here) are summarized in Fig. 7. However, we have to keep in mind that our calculation of the inelastic mean free path is based on the assumption that diffraction effects are negligible and that the applied model includes continuous damping of photoelectrons that are emitted from discrete layers of the solid, which might cause problems when very thin layers are considered.

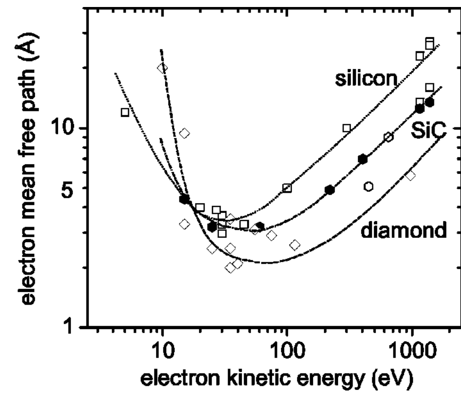

FIG. 7. Electron mean free path as a function of electron energy for the three materials, silicon (open squares, Refs. 53 and 54), silicon carbide (open hexagons from Ref. 13, filled hexagons from this work), and diamond (open diamonds, Refs. 55–57). The lines are guides to the eye.

E. Thermally induced hydrogen desorption and subsequent surface reactions on 6*H*-SiC(0001):H

Figure 8 shows Si 2*p* and C 1*s* core-level spectra of a hydrogenated 6*H*-SiC(0001) surface taken after preparation and after subsequent heating to temperatures of up to 820 °C. Before heating, the core-levels show the behavior discussed in Sec. III C. Note that the hydrocarbon contamination is increased with respect to the spectrum shown in Fig. 6 due to a longer storage time in the vacuum transport vessel. Annealing the sample to 640 °C has essentially no

TABLE IV. Fit parameters obtained for the C 1*s* core-level spectra of hydrogenated 6*H*-SiC(0001). The binding energy is given with respect to the bulk component.

C 1*s*	$\hbar\omega = 350$ eV, $\lambda_{eff} = 3.0$ Å			$\hbar\omega = 510$ eV, $\lambda_{eff} = 4.6$ Å		
Label in Fig. 6	B_C	S_C1	S_C2	B_C	S_C1	S_C2
E_b (eV)	0	0.46 ± 0.02	2.12 ± 0.10	0	0.48 ± 0.02	2.27 ± 0.13
$I(S_C1{,}2)/I(B_C)$		0.07 ± 0.01	0.06 ± 0.01		0.06 ± 0.01	0.04 ± 0.01
ω_G (eV)	0.54 ± 0.02	0.65 ± 0.03	1.16 ± 0.08	0.57 ± 0.02	0.63 ± 0.03	1.24 ± 0.11
ω_L (eV)	0.19 ± 0.03	0.19 ± 0.03	0.19 ± 0.03	0.19 ± 0.03	0.19 ± 0.03	0.19 ± 0.03
Assignment	SiC bulk	Si_3C-H	C_xH_y	SiC bulk	Si_3C-H	C_xH_y

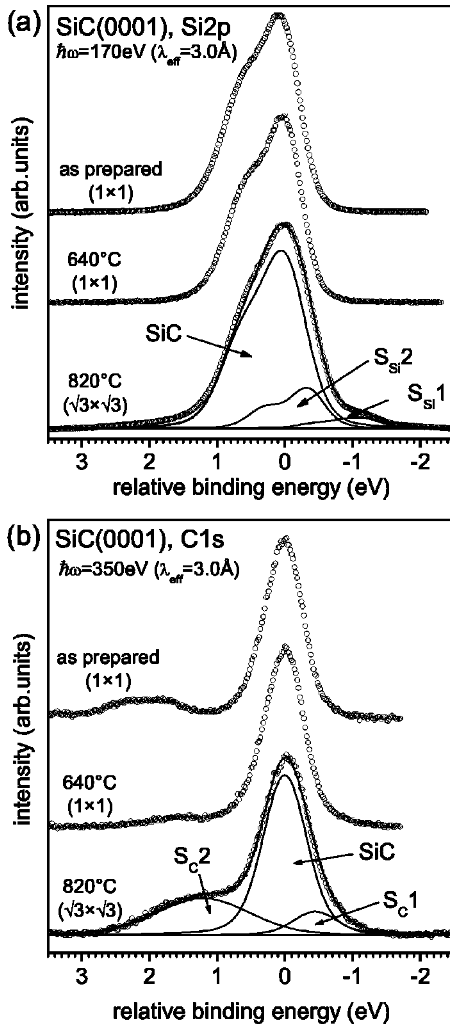

FIG. 8. Si $2p$ (a) and C $1s$ (b) core-level spectra of hydrogenated $6H$-SiC(0001) after annealing in UHV.

effect on the Si $2p$ spectrum. In the C $1s$ spectrum the component due to the hydrocarbon contamination becomes weaker and shifts 0.6 eV towards the SiC bulk component. This indicates a partial desorption of the contaminants accompanied by a decomposition of the remaining hydrocarbons. The surface symmetry remains (1×1). Annealing to temperatures above 750 °C (not shown) gradually leads to the formation of a $(\sqrt{3}\times\sqrt{3})R30°$ reconstruction, which is fully developed at 820 °C.

The Si $2p$ and C $1s$ spectra taken after annealing to 820 °C are also shown in Fig. 8 together with the results of a deconvolution of the spectra. The best fit parameters are collected in Tables V and VI for the Si $2p$ and C $1s$ core-levels, respectively, measured with different surface sensitivities. In the Si $2p$ spectrum two new chemically shifted components labeled $S_{\mathrm{Si}}1$ and $S_{\mathrm{Si}}2$ can be observed. The intensity variation of these two components upon changing the probe depth (see Table V) reveals their surface nature. These components are characteristic of the Si-rich $(\sqrt{3}\times\sqrt{3})R30°$ reconstruction.[13] Their chemical shifts of -0.33 ± 0.04 and -1.10 ± 0.06 eV with respect to the SiC bulk component (see Table V) are in excellent agreement with the observations of Johansson *et al.*[13] According to the structural model which was determined by LEED,[22] the signal $S_{\mathrm{Si}}1$ at -0.33 eV is due to the Si atoms of the topmost SiC bilayer for which the more electronegative binding partner carbon is replaced by Si adatoms. These adatoms which give rise to the second chemically shifted component ($S_{\mathrm{Si}}2$) reside in T_4 position and each of them is bound to three Si atoms of the topmost SiC bilayer thus forming the $(\sqrt{3}\times\sqrt{3})R30°$ superstructure. In addition, we note that the fit is not perfect at the higher binding-energy side, where a weak tailing can be observed. This is most likely due to the onset of oxidation of this strongly reactive surface.[59]

The C $1s$ core-level of the Si-rich $(\sqrt{3}\times\sqrt{3})R30°$ reconstruction is also made up of at least three components, which is in agreement with the observations of Johansson *et al.*[13] Two components are found to be due to emission from the surface (see Table VI) and they are labeled $S_{\mathrm{C}}1$ and $s_{\mathrm{C}}2$. Their binding energies are (-0.43 ± 0.07) eV and (1.20 ± 0.10) eV relative to the bulk component, respectively. The component $S_{\mathrm{C}}1$ is ascribed to carbon atoms of the first bilayer that are affected by the surface modifications. This seems reasonable, since due to the silicon-rich surface the effective electronegativity of all interface silicon atoms appears reduced, which causes a small chemical shift of the component which corresponds to the next neighboring carbon atoms to lower binding energy. Some confusion was caused in the past because of the existence of the second surface carbon component $S_{\mathrm{C}}2$, which could not be explained within the structural model of the $(\sqrt{3}\times\sqrt{3})R30°$ reconstruction. Johansson *et al.*[13] discussed several possible bonding configurations but none of these could describe the real bonding arrangement as finally determined by an LEED study.[22] Tautz *et al.*[23] concluded that the component $S_{\mathrm{C}}2$

TABLE V. Fit parameters obtained for the Si $2p$ core-level spectra of hydrogenated $6H$-SiC(0001) after annealing to 820 °C and conversion to the Si-rich $(\sqrt{3}\times\sqrt{3})$ reconstruction. The binding energy is given with respect to the bulk component.

Si $2p$	$\hbar\omega=170$ eV, $\lambda_{eff}=3.0$ Å			$\hbar\omega=350$ eV, $\lambda_{eff}=4.6$ Å		
Label in Fig. 8(a)	B_{Si}	$S_{\mathrm{Si}}1$	$S_{\mathrm{Si}}2$	B_{Si}	$S_{\mathrm{Si}}1$	$S_{\mathrm{Si}}2$
E_b (eV)	0	-1.11 ± 0.05	-0.33 ± 0.04	0	-1.08 ± 0.05	-0.31 ± 0.03
$I(S_{\mathrm{Si}}1,2)/I(B_{\mathrm{Si}})$		0.06 ± 0.01	0.20 ± 0.02		0.04 ± 0.01	0.15 ± 0.02
ω_G (eV)	0.67 ± 0.03	0.62 ± 0.03	0.51 ± 0.02	0.62 ± 0.03	0.64 ± 0.03	0.58 ± 0.02
ω_L (eV)	0.14 ± 0.03	0.14 ± 0.03	0.14 ± 0.03	0.14 ± 0.03	0.14 ± 0.03	0.14 ± 0.03
Assignment	SiC bulk	$\mathrm{Si}_{T_4-\mathrm{adatom}}$	$\mathrm{C}_{\mathrm{interface}}$	SiC bulk	$\mathrm{Si}_{T_4-\mathrm{adatom}}$	$\mathrm{C}_{\mathrm{interface}}$

TABLE VI. Fit parameters obtained for the C 1s core-level spectra of hydrogenated 6H-SiC(0001) after annealing to 820 °C and conversion to the Si-rich ($\sqrt{3}\times\sqrt{3}$) reconstruction. The binding energy is given with respect to the bulk component.

C 1s	$\hbar\omega$=350 eV, λ_{eff}=3.0 Å			$\hbar\omega$=510 eV, λ_{eff}=4.6 Å		
Label in Fig. 8(b)	B_C	S_C1	S_C2	B_C	S_C1	S_C2
E_b (eV)	0	−0.45±0.02	1.25±0.05	0	−0.40±0.05	1.15±0.05
$I(S_C1,2)/I(B_C)$		0.14±0.02	0.42±0.04		0.06±0.01	0.18±0.02
ω_G (eV)	0.66±0.03	0.66±0.03	1.47±0.10	0.61±0.03	0.69±0.03	1.45±0.10
ω_L (eV)	0.20±0.03	0.20±0.03	0.20±0.03	0.20±0.03	0.20±0.03	0.20±0.03
Assignment	SiC bulk	$C_{interface}$	C_{excess}	SiC bulk	$C_{interface}$	C_{excess}

must be of extrinsic nature due to contamination from the residual gas of their vacuum chamber, since they observed a time-dependent increase.

However, we propose that in principle one has to consider how the ($\sqrt{3}\times\sqrt{3}$)$R30°$ reconstructed surface is prepared. The method of Johansson *et al.*[13] and our method have in common that the reconstruction is prepared by annealing an unreconstructed surface at elevated temperatures. In both cases no extra silicon is provided to form the reconstruction. Tautz *et al.*[23] evaporated silicon onto the surface until a (3×3) Si-rich reconstruction was observed. The ($\sqrt{3}\times\sqrt{3}$)$R30°$ reconstruction then forms during annealing at temperatures between 900 °C and 950 °C, i.e., during removal of excess silicon from the surface via thermal desorption. The latter method is supposed to be more convenient, since the extra silicon which is necessary to form the silicon-rich reconstruction is provided by an evaporation source.

In our case the starting point is a surface covered with a monolayer of hydrogen atoms. Annealing leads to hydrogen desorption and the formation of the ($\sqrt{3}\times\sqrt{3}$)$R30°$ reconstruction although no surplus silicon for the formation of the Si adatoms is provided. But where does the extra silicon come from? The key answer is that the reconstructed surface is inhomogeneous and only a part of it is covered by the ($\sqrt{3}\times\sqrt{3}$)$R30°$ reconstruction. The ordered areas, however, are large enough to lead to a ($\sqrt{3}\times\sqrt{3}$)$R30°$ diffraction pattern, i.e., their dimension must exceed some few hundred angstroms, which is the typical transfer width of a LEED experiment. Any silicon enrichment in some part of the surface must necessarily be accompanied by a silicon depletion in other regions. As we have seen in our spectra both $S_{Si}1$ and S_C2 components are located at the surface and their intensities increase simultaneously as soon as the ($\sqrt{3}\times\sqrt{3}$)$R30°$ structure starts to develop. Therefore, at least a major part of the S_C2 signal together with the $S_{Si}1$ signal must originate in a dissociation of SiC at the surface. The resulting Si atoms diffuse along the surface to occupy T_4 sites in order to minimize the surface free energy leaving behind carbon-rich surface regions that are covered by elemental carbon. Since the dissociation process produces both, silicon-rich and carbon-rich areas on the surface at the same time we like to call it a disproportionation, although no formal change of the oxidation state of Si and C occurs. The above described scenario is supported when the relative binding energies of S_C2 and $S_{Si}1$ are considered. The chemical shift of S_C2 amounts to 1.25±0.05 eV and is typical of elemental carbon, since the replacement of one carbon atom of a C_4-C tetrahedron by one silicon atom yields about 0.35 eV smaller binding energy for the center carbon atom which adds to about 1.4 eV.[58] The chemical shift of $S_{Si}1$ amounts to −1.15±0.05 eV and fits well to the expected shift of −1.2 eV for elemental silicon with respect to SiC. The dangling bond (db) in the Si_3Si-db environment can be interpreted as a fourth Si atom in a Si_3Si-Si tetrahedron, since the effective electronegativity of the center Si atom in a Si_3Si-db and in a Si_3Si-Si environment is expected to be equal.

The same mechanism for the formation of the ($\sqrt{3}\times\sqrt{3}$)$R30°$ structure holds in principle when a wet-chemically prepared SiC(0001) surface is used as starting point as was done by Johansson *et al.*[13] The difference compared to our measurements is the fact that the wet-chemically treated surfaces of Johansson *et al.* contained a large amount of hydrocarbon contamination so that the observation of the simultaneous formation of elemental species was hindered. However, it remains unclear if and to what extent the S_C2 species contain sp^3 and sp^2 bonding arrangements, i.e., whether it is partially graphitic or not. Finally, we note that the formation of S_C2 is completely suppressed when the Si evaporation method is applied as was successfully shown by Amy *et al.* for the Si-rich (3×3) reconstruction.[3]

It is interesting to note that in our experiments the ($\sqrt{3}\times\sqrt{3}$)$R30°$ periodicity started to develop at 750 °C whereas the preparation methods mentioned above require temperatures above 900 °C.[3,13,23] We explain this with a lower desorption temperature for hydrogen as compared to the desorption temperature of oxygen and/or the temperature at which Si sublimation occurs. Figure 9 shows the hydrogen coverage as a function of annealing temperature as determined by FTIR-ATR. As can be seen from that figure, rapid hydrogen desorption is observed starting at around 700 °C and is completed at 750 °C, at which temperature the development of the ($\sqrt{3}\times\sqrt{3}$)$R30°$ reconstruction was observed. Obviously, annealing of the hydrogenated surface to temperatures between 700 °C and 750 °C provides the activation energy for both hydrogen desorption and formation of the ($\sqrt{3}\times\sqrt{3}$)$R30°$ reconstruction by the mechanism alluded to above, i.e., disproportionation of SiC.

F. Thermally induced hydrogen desorption and subsequent surface reactions on 6H-SiC(000$\bar{1}$):H

The effect of annealing in UHV on the core-level spectra of hydrogen-terminated 6H-SiC(000$\bar{1}$) can be seen in Fig.

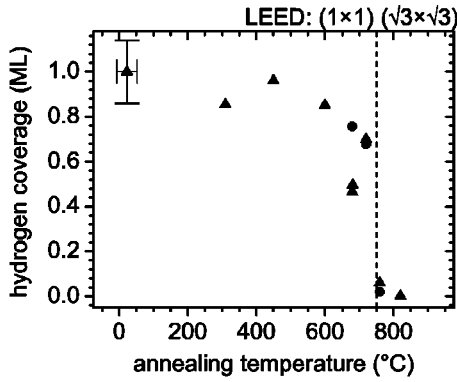

FIG. 9. Hydrogen coverage (in monolayers) as determined from the signal strength of the Si-H stretch mode in FTIR-ATR as a function of annealing temperature. The hydrogen coverage was determined from the relative signal strength before and after annealing the sample in UHV.

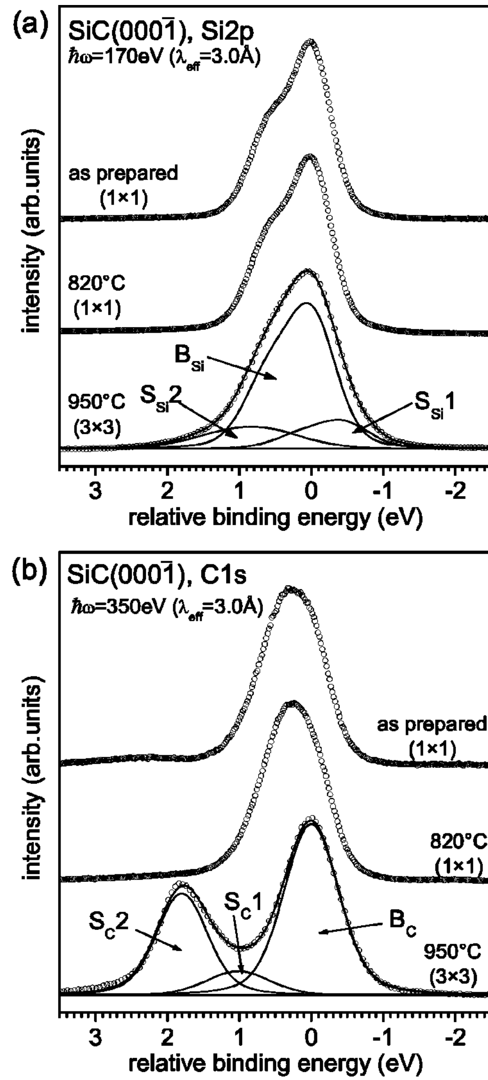

FIG. 10. Si $2p$ (a) and C $1s$ (b) core-level spectra of hydrogenated $6H$-SiC($000\bar{1}$) after annealing in UHV.

10. The line shape of the Si $2p$ core-level remains unaffected up to 820 °C. In the C $1s$ core-level spectrum the only variation that is observable is a slight reduction of hydrocarbon contamination. Additionally, we observe that the relative binding energy of this contamination component shifts closer to the bulk line by 0.6 eV. As already proposed for $6H$-SiC(0001) (see Sec. III E) this can be explained by a partial decomposition of remaining hydrocarbons at the surface. The surface periodicity remained (1×1) as was checked by LEED. Increasing the temperature to 950 °C leads to the formation of a (3×3) reconstruction which is accompanied by clear changes in the shape of the Si $2p$ and C $1s$ core-level spectra. Both spectra can be deconvoluted using three components. An example of such a deconvolution is also shown in Fig. 10. The best fit parameters for surface and bulk sensitive Si $2p$ and C $1s$ core-level spectra taken after annealing to 950 °C are compiled in Tables VII and VIII, respectively.

As we have seen in the case of the SiC(0001) surface, hydrogen desorption commences between 700 °C and 750 °C, the same temperature at which the $(\sqrt{3}\times\sqrt{3})R30°$ reconstruction is formed. In contrast to that, first signs of hydrogen desorption on $6H$-SiC($000\bar{1}$) are already seen after annealing at 670 °C. In the valence-band spectra shown in Fig. 11, a small but clear peak develops above the valence-band maximum in the energy gap of 6H-SiC, which is labeled D_C. The location of D_C is typical for a dangling bond state. A comparable dangling bond state was previously observed on the silicate adlayer reconstruction on $6H$-SiC($000\bar{1}$).[27] The observation of D_C indicates that hydrogen desorption on $6H$-SiC($000\bar{1}$) is possible without immediate reconstruction of surface. This is probably due to the stronger localization of the carbon valence orbitals, which causes unfavorable bond angles and lengths on reconstructed

TABLE VII. Fit parameters obtained for the Si $2p$ core-level spectra of hydrogenated $6H$-SiC($000\bar{1}$) after annealing to 950 °C and conversion to the Si-rich (3×3) reconstruction. The binding energy is given with respect to the bulk component.

Si $2p$	$\hbar\omega=170$ eV, $\lambda_{eff}=3.0$ Å			$\hbar\omega=350$ eV, $\lambda_{eff}=4.6$ Å		
Label in Fig. 10(a)	B_{Si}	$S_{\text{Si}}1$	$S_{\text{Si}}2$	B_{Si}	$S_{\text{Si}}1$	$S_{\text{Si}}2$
E_b (eV)	0	-0.45 ± 0.04	0.67 ± 0.06	0	-0.47 ± 0.05	0.59 ± 0.06
$I(S_{\text{Si}}1,2)/I(B_{\text{Si}})$		0.20 ± 0.04	0.21 ± 0.04		0.08 ± 0.01	0.08 ± 0.01
ω_G (eV)	0.77 ± 0.03	0.71 ± 0.03	1.24 ± 0.07	0.69 ± 0.04	0.69 ± 0.05	1.37 ± 0.09
ω_L (eV)	0.15 ± 0.03	0.15 ± 0.03	0.15 ± 0.03	0.15 ± 0.03	0.15 ± 0.03	0.15 ± 0.03
Assignment	SiC bulk	$\text{Si}_{\text{excess}}$	SiO_z	SiC bulk	$\text{Si}_{\text{excess}}$	SiO_z

TABLE VIII. Fit parameters obtained for the C $1s$ core-level spectra of hydrogenated $6H$-SiC($000\bar{1}$) after annealing to 950 °C and conversion to the Si-rich (3×3) reconstruction. The binding energy is given with respect to the bulk component.

C $1s$	$\hbar\omega=350$ eV, $\lambda_{eff}=3.0$ Å			$\hbar\omega=510$ eV, $\lambda_{eff}=4.6$ Å		
Label in Fig. 10(b)	B_C	S_C1	S_C2	B_C	S_C1	S_C2
E_b (eV)	0	1.02 ± 0.06	1.80 ± 0.03	0	1.07 ± 0.06	1.83 ± 0.03
$I(S_C1,2)/I(B_C)$		0.16 ± 0.02	0.56 ± 0.04		0.10 ± 0.01	0.41 ± 0.03
ω_G (eV)	0.77 ± 0.03	0.91 ± 0.05	0.71 ± 0.02	0.78 ± 0.03	0.85 ± 0.06	0.73 ± 0.03
ω_L (eV)	0.23 ± 0.03	0.23 ± 0.03	0.23 ± 0.03	0.23 ± 0.03	0.23 ± 0.03	0.23 ± 0.03
Assignment	SiC bulk	$C_{adlayer}$	$C_{interface}$	SiC bulk	$C_{adlayer}$	$C_{interface}$

surfaces.[20] In addition, the annealing step leads to a change in band bending which manifests itself in a shift of the whole spectrum to lower binding energy by 1.0 eV. Of course the question arises, why the core-level spectra after annealing at 820 °C are so similar to the ones of the as-prepared sample (see Fig. 10). The unaltered shape of the Si $2p$ core-level after hydrogen desorption which is most likely complete after annealing at 820 °C fulfills the expectation in that C-H bonds merely affect the topmost carbon layer but hardly the electronic structure of the silicon atoms underneath. As a consequence, hydrogen desorption will have no effect on the Si $2p$ core-level shape. On the other hand, it is difficult to estimate how the C-H component of the C $1s$ core level evolves upon hydrogen desorption. In principle, the chemical shift of unsaturated surface carbon atoms in an Si_3C-db environment should not be much different from that in a Si_3C-C environment, since in the latter case the same valence charge is transferred between both carbon atoms as in the former, namely, zero. As a result, the binding energy of the unsaturated surface carbon atoms is expected at 0.35 eV higher binding relative to the bulk component.[58] This would explain why the C $1s$ spectra remain unchanged upon hydrogen desorption: the chemical shift of hydrogenated surface carbon amounts to (0.47 ± 0.02) eV (Sec. III B) and has to be compared with the estimated shift of 0.35 eV. It is not possible to resolve the expected binding energy change of about 0.1 eV in the presence of the large Gaussian widths of the core-level spectra.

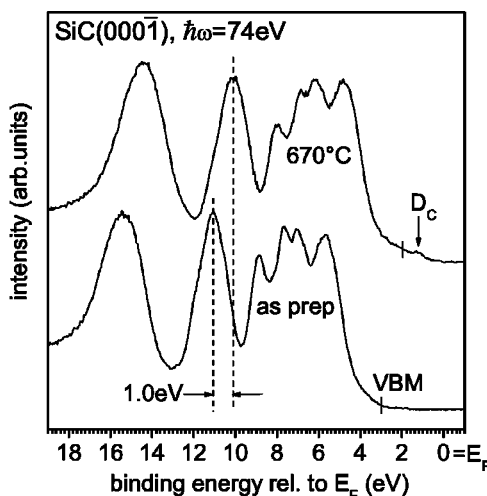

FIG. 11. Valence-band spectra of hydrogenated $6H$-SiC($000\bar{1}$) directly after preparation and after annealing in UHV to 670 °C.

The C $1s$ core-levels of the (3×3) reconstructed $6H$-SiC($000\bar{1}$) surface have been deconvoluted into three components [see Fig. 10(b) and Table VIII]. Two surface components S_C1 and S_C2 are necessary to fit the spectrum adequately. This was also reported by Johansson *et al.*[25] However, the component in their work which is equivalent to our S_C1 component was much broader ($\omega_G=2.1$ eV). This may be due to the fact that they started from a wet-chemically prepared surface which was covered by a considerable amount of hydrocarbons.[25] As discussed above, the hydrocarbons decompose partially during annealing and may obscure the C $1s$ spectral shape in the work of Johansson *et al.*[25] The photon energy dependence of the intensity ratio of the two components (see Table VIII) suggests that the C atoms corresponding to S_C1 are located above the C-atoms corresponding to S_C2, which in turn are located above the carbon atoms of the bulk. This again is in contrast to the work of Johansson *et al.*,[25] who concluded that C atoms corresponding to S_C2 are located above C atoms corresponding to S_C1. This disagreement may also be due to the larger initial hydrocarbon contamination on their samples. Therefore we propose that the (3×3) structure is made up of carbon adatoms on top of carbon interface layer. In our study the intensity ratio of S_C1 to S_C2 is around 0.3 which indicates that one carbon atom corresponding to S_C1 is located above three to four carbon atoms corresponding to S_C2. However, proposing a more detailed structural model based on the data at hand would be too speculative.

In the Si $2p$ core-level spectra taken after annealing to 950 °C [see Fig. 10(a) and Table VII], we observe two chemically shifted components $S_{Si}1$ at lower and $S_{Si}2$ at higher binding energy relative to the bulk component. Component $S_{Si}1$ can be explained in a similar way as the component S_C2 in the C $1s$ spectra of the $(\sqrt{3}\times\sqrt{3})R30°$ reconstruction of SiC(0001), i.e., excess Si which is left behind during the formation of the carbon-rich (3×3) structure again following disproportionation of SiC. The second surface component $S_{Si}2$ is located at 0.63 eV higher binding energy which suggests the onset of oxidation of the Si enriched regions and formation of Si^+. It is well known from Si-rich reconstructions of SiC surfaces that they are susceptible to oxidation. For example, the Si-rich $(\sqrt{3}\times\sqrt{3})R30°$

reconstructed SiC(0001) surface was observed to be easily oxidized even at liquid-nitrogen temperature.[59] The observation of surface components in the Si $2p$ spectra of the (3×3) reconstructed $6H$-SiC$(000\bar{1})$ surface is also in contrast to the work of Johansson *et al.*,[25] who have not observed any surface components in their Si $2p$ spectra. Again the reason for this discrepancy is most likely the initial hydrocarbon contamination on the wet-chemically prepared samples, which may yield the carbon necessary for the (3×3) structure without disproportionation of SiC.

IV. CONCLUSION

In this paper we present results of photoelectron spectroscopy on hydrogenated hexagonal SiC surfaces using synchrotron radiation. On $6H$-SiC$(000\bar{1})$ a chemically shifted surface component due to carbon atoms in a Si_3C-H environment could be identified. As expected, the corresponding Si $2p$ core-level does not exhibit chemically shifted components. The Si $2p$ core-level spectra of hydrogenated $6H$-SiC(0001) suggest the presence of a chemically shifted surface component due to C_3Si-H, but a definite assignment was not possible because of the intrinsically large Gaussian width of the core-levels that are generally observed on SiC surfaces.

In addition, the thermally induced hydrogen desorption and subsequent formation of surface reconstructions was studied. The advantage of the hydrogenated surfaces is that they provide a starting point at which the Si:C ratio of the surface is ideally 1:1. In this way the formation of the Si-rich $(\sqrt{3}\times\sqrt{3})R30°$ reconstruction on SiC(0001) and the carbon-rich (3×3) reconstruction on SiC$(000\bar{1})$ was studied. On SiC(0001) thermal desorption of hydrogen from the SiC(0001) surface occurs between 700 °C and 750 °C and is accompanied by the formation of the Si-rich $(\sqrt{3}\times\sqrt{3})R30°$ reconstruction. The core-level spectra are in good agreement with the literature. The origin of the surface component S_C2 in the C $1s$ core-level spectra has been identified as due to excess carbon, which originates from a disproportionation of SiC. On $6H$-SiC$(000\bar{1})$ first signs of thermal hydrogen desorption are seen at 670 °C where the (1×1) periodicity of the surface is still conserved. At 950 °C the surface undergoes a transition to the (3×3) reconstructed surface. The C $1s$ core-levels suggest a structure in which C adatoms are located above the topmost carbon layer. As for SiC(0001), a disproportionation of SiC is necessary to provide carbon atoms forming the reconstruction leaving behind Si enriched areas on the surface. As a consequence, the $(\sqrt{3}\times\sqrt{3})R30°$ reconstructed SiC(0001) and the (3×3) reconstructed SiC$(000\bar{1})$ surfaces formed from wet-chemically prepared or hydrogenated surfaces have to be considered inhomogeneous. Using them as starting points for device production by depositing materials on top of them seems inappropriate.

ACKNOWLEDGMENTS

This work was supported by the Deutsche Forschungsgemeinschaft through Grant No. SFB 292. We thank Dr. R. Graupner and Dr. J. Ristein for fruitful discussions. We also express our gratitude for support by the people from BESSY II, especially by Dr. W. Braun, and by Dr. W. Mahler and Dr. B. Zada from the FHI.

*Corresponding author. Email address: thomas.seyller@physik.uni-erlangen.de

[1] M.A. Kulakov, G. Henn, and B. Bullemer, Surf. Sci. **346**, 49 (1996).
[2] V.A. Gasparov, M. Riehl-Chudoba, B. Schröter, and W. Richter, Europhys. Lett. **51**, 527 (2000).
[3] F. Amy, H. Enriquez, P. Soukiassian, P.F. Storino, Y.J. Chabal, A.J. Mayne, G. Dujardin, Y.K. Hwu, and C. Brylinski, Phys. Rev. Lett. **86**, 4342 (2001).
[4] J. Schardt, J. Bernhardt, U. Starke, and K. Heinz, Phys. Rev. B **62**, 10 335 (2000).
[5] S. Nakanishi, H. Tokutaka, K. Nishimori, S. Kishida, and N. Ishihara, Appl. Surf. Sci. **41**, 44 (1989).
[6] R. Kaplan, Surf. Sci. **215**, 111 (1989).
[7] U. Starke, Phys. Status Solidi B **202**, 475 (1997).
[8] J. Furthmüller, F. Bechstedt, H. Hüsken, B. Schröter, and W. Richter, Phys. Rev. B **58**, 13 712 (1998).
[9] U. Starke, J. Bernhardt, J. Schardt, and K. Heinz, Surf. Rev. Lett. **6**, 1129 (1999).
[10] K. Heinz, U. Starke, J. Bernhardt, and J. Schardt, Appl. Surf. Sci. **162-163**, 9 (2000).
[11] A.J. van Bommel, J.E. Crombeen, and A. van Tooren, Surf. Sci. **48**, 463 (1975).
[12] F. Owman and P. Martensson, Surf. Sci. **330**, L639 (1995).
[13] L.I. Johansson, F. Owman, and P. Martensson, Phys. Rev. B **53**, 13 793 (1996).
[14] L.I. Johansson, F. Owman, P. Martensson, C. Persson, and U. Lindefelt, Phys. Rev. B **53**, 13 803 (1996).
[15] L.I. Johansson, F. Owman, and P. Martensson, Surf. Sci. **360**, L478 (1996).
[16] V. van Elsenbergen, O. Janzen, and W. Mönch, Mater. Sci. Eng., B **B46**, 366 (1997).
[17] J.M. Themlin, I. Forbeaux, V. Langlais, H. Belkhir, and J.M. Debever, Europhys. Lett. **39**, 61 (1997).
[18] J.E. Northrup and J. Neugebauer, Phys. Rev. B **52**, R17 001 (1995).
[19] J.E. Northrup and J. Neugebauer, Phys. Rev. B **57**, R4230 (1998).
[20] M. Sabisch, P. Krüger, and J. Pollmann, Phys. Rev. B **55**, 10 561 (1997).
[21] V. Ramachandran and R.M. Feenstra, Phys. Rev. Lett. **82**, 1000 (1999).
[22] U. Starke, J. Schardt, J. Bernhardt, M. Franke, and K. Heinz, Phys. Rev. Lett. **82**, 2107 (1999).
[23] F.S. Tautz, S. Sloboshanin, U. Starke, and J.A. Schaefer, Surf. Sci. **470**, L25 (2000).
[24] M. Rohlfing and J. Pollmann, Phys. Rev. Lett. **84**, 135 (2000).
[25] L.I. Johansson, P.A. Glans, and N. Hellgren, Surf. Sci. **405**, 288 (1998).

[26] J. Bernhardt, J. Schardt, U. Starke, and K. Heinz, Appl. Phys. Lett. **74**, 1084 (1999).
[27] M. Hollering *et al.*, Surf. Sci. **442**, 531 (1999).
[28] M. Hollering, N. Sieber, J. Ristein, L. Ley, J.D. Riley, R.C.G. Leckey, F.P. Leisenberger, and F.P. Netzer, Mater. Sci. Forum **338-342**, 387 (2000).
[29] N. Sieber, M. Hollering, J. Ristein, and L. Ley, Mater. Sci. Forum **338-342**, 391 (2000).
[30] W. Lu, P. Krüger, and J. Pollmann, Phys. Rev. B **61**, 13 737 (2000).
[31] W.C. Lu, P. Krüger, and J. Pollmann, Mater. Sci. Forum **338-342**, 349 (2000).
[32] N. Sieber, T. Seyller, R. Graupner, L. Ley, R. Mikalo, P. Hoffmann, D. Batchelor, and D. Schmeißer, Mater. Sci. Forum **389-393**, 717 (2002).
[33] E. Yablonovitch, D.L. Allara, C.C. Chang, T. Gmitter, and T.B. Bright, Phys. Rev. Lett. **57**, 249 (1986).
[34] D. Gräf, M. Grundner, R. Schulz, and L. Mühlhoff, J. Appl. Phys. **68**, 5155 (1990).
[35] N. Sieber, T. Seyller, R. Graupner, L. Ley, R. Mikalo, P. Hoffmann, D.R. Batchelor, and D. Schmeißer, Appl. Surf. Sci. **184**, 280 (2001).
[36] U. Starke, C. Bram, P.R. Steiner, W. Hartner, L. Hammer, K. Heinz, and K. Müller, Appl. Surf. Sci. **89**, 175 (1995).
[37] M. Hollering, B. Mattern, F. Maier, L. Ley, A.P.J. Stampfl, J. Xue, J.D. Riley, and R.C.G. Leckey, Mater. Sci. Forum **264-268**, 331 (1998).
[38] H. Tsuchida, I. Kamata, and K. Izumi, Appl. Phys. Lett. **70**, 3072 (1997).
[39] H. Tsuchida, I. Kamata, and K. Izumi, Jpn. J. Appl. Phys., Part 2 **36**, L699 (1997).
[40] H. Tsuchida, I. Kamata, and K. Izumi, Mater. Sci. Forum **264-268**, 351 (1998).
[41] H. Tsuchida, I. Kamata, and K. Izumi, J. Appl. Phys. **85**, 3569 (1999).
[42] C. Hallin, A.S. Bakin, F. Owman, P. Mårtensson, O. Kordina, and E. Janzén, Inst. Phys. Conf. Ser. **142**, 613 (1996).
[43] F. Owman, C. Hallin, P. Mårtensson, and E. Janzén, J. Cryst. Growth **167**, 391 (1996).
[44] N. Sieber, B.F. Mantel, T. Seyller, J. Ristein, L. Ley, T. Heller, D.R. Batchelor, and D. Schmeißer, Appl. Phys. Lett. **78**, 1216 (2001).
[45] N. Sieber, T. Stark, T. Seyller, L. Ley, C. Zorman, and M. Mereghany, Appl. Phys. Lett. **80**, 4726 (2002).
[46] N. Sieber, B.F. Mantel, T. Seyller, J. Ristein, and L. Ley, Diamond Relat. Mater. **10**, 1291 (2001).
[47] N. Sieber, T. Seyller, B.F. Mantel, J. Ristein, and L. Ley, Mater. Sci. Forum **353-356**, 223 (2001).
[48] N. Sieber, T. Seyller, L. Ley, M. Polcik, D. James, J.D. Riley, and R.G.C. Leckey, Mater. Sci. Forum **389-393**, 713 (2002).
[49] D. Shirley, Phys. Rev. B **5**, 4079 (1972).
[50] L.I. Johansson, H.I.P. Johansson, and K.L. Hakansson, Phys. Rev. B **48**, 14 520 (1993).
[51] K.L. Hakansson, H.I.P. Johansson, and L.I. Johansson, Phys. Rev. B **48**, 2623 (1993).
[52] C.J. Karlsson, F. Owman, E. Landemark, Y.C. Chao, P. Martensson, and R.I.G. Uhrberg, Phys. Rev. Lett. **72**, 4145 (1994).
[53] F.J. Himpsel, F.R. McFeely, A. Taleb-Ibrahimi, J.A. Yarmoff, and G. Hollinger, Phys. Rev. B **38**, 6084 (1988).
[54] G.K. Wertheim, D.M. Riffe, J.E. Rowe, and P.H. Citrin, Phys. Rev. Lett. **67**, 120 (1991).
[55] B.B. Pate, M. Oshima, J.A. Silberman, G. Rossi, I. Lindau, and W.E. Spicer, J. Vac. Sci. Technol. A **2**, 957 (1984).
[56] J.F. Morar, F.J. Himpsel, G. Hollinger, J.L. Jordan, G. Hughes, and F.R. McFeely, Phys. Rev. B **33**, 1340 (1986).
[57] R. Graupner, Ph.D. thesis, University of Erlangen-Nürnberg, 1997.
[58] R.C. Fang and L. Ley, Phys. Rev. B **40**, 3818 (1989).
[59] C. Virojanadara and L. Johansson, Surf. Sci. **519**, 73 (2002).
[60] W. Kern and D.A. Puotinen, RCA Rev. **31**, 187 (1970).